Sensors and Materials, Vol. 36, No. 3 (2024) 945–955
MYU Tokyo

S & M 3573

Finger-vein Secure Access Based on Lightweight Dual-attention Convolutional Neural Network for Quality Distance Education

Liang-Ying Ke[1] and Chih-Hsien Hsia[1,2*]

[1]Department of Computer Science and Information Engineering, National Ilan University, Yilan, Taiwan
[2]Department of Business Administration, Chaoyang University of Technology, Taichung, Taiwan

(Received January 13, 2024; accepted February 28, 2024)

Keywords: deep learning, finger-vein recognition, margin-based loss function, lightweight network, quality education

As global average fertility rates decline annually, a crisis brought by declining birthrates gradually emerges, further impacting the existing education system. In response to the impact of declining birthrates on education, countries have recently accelerated the development of distance learning. Distance learning provides guaranteed access to comprehensive and quality education while encouraging continuous learning opportunities for everyone. However, the identity recognition technology used in the current distance learning platform seldom addresses the problem of inconsistent image quality in actual scenarios, making it difficult to ensure the practical application of the model. To solve these issues, we propose a lightweight dual-attention convolutional neural network (LDA-FV) constructed through a dual attention-based inverted residual block (DA-IRB) and implemented using an adaptive margin loss (AML) function for finger-vein recognition. This method not only extracts effective finger-vein features through DA-IRB but also adjusts the training difficulty in accordance with the image quality. Furthermore, owing to its lightweight design, the model can be more flexibly deployed on existing hardware devices (e.g., mouse) in distance education scenarios. The experimental results of this study indicate that the proposed method effectively enhanced the model's recognition capability using the finger-vein database of the University Sains Malaysia (FV-USM) and the PLUSVein dorsal-palmar finger-vein (PLUSVein-FV3) public database, achieving correct identification rates (CIRs) of 99.90% and 97.50%, respectively.

1. Introduction

According to a 2023 report by the United Nations Population Fund, the global average birth rate per woman has significantly declined from 5.0 in 1950 to 2.3 in 2021.(1) Although the current global birth rate remains above the 2.1 fertility replacement rate, there is a declining trend of sub-replacement fertility, leading to the predicament of lower enrollment in schools, resulting in their closure or consolidation.(2) The reduction in the number of students has forced some schools to pass on the operational costs to their current students, putting them under the pressure of high

*Corresponding author: e-mail: hsiach@niu.edu.tw
https://doi.org/10.18494/SAM4858

ISSN 0914-4935
https://myukk.org/

tuition fees and even forcing them to discontinue their studies.[3] Furthermore, the COVID-19 pandemic in 2020 exacerbated the phenomenon of students discontinuing their education.[4] To address the impact of the pandemic, countries accelerated the development of distance learning, necessitating the conversion of many courses to online platforms for teaching and examinations.[5] However, with teaching shifted to virtual classrooms, traditional classroom norms and group dynamics that kept students focused and restricted their behavior became less effective, leading to the possibility of cheating during exams.[6] In a previous study, this problem was addressed by proposing various anticheating systems.[7] Additionally, identity recognition technology is essential to maintain the quality, fairness, and security of distance learning. Using identity recognition not only ensures that students participating in online courses and exams are not imposters,[8] but it also prevents unauthorized access to personal data and enables teaching platforms to offer a more personalized learning experience based on individual student progress and preferences.[9]

In recent years, with the development of computer vision (CV) and deep learning technologies, and driven by the COVID-19 pandemic, the intelligent learning industry market has become increasingly active.[10] Concurrently, the number of research studies on biometric feature-based identity recognition has also increased.[11] Among these, the second generation of biometrics recognition technology, which uses vein features for identity recognition, has garnered significant attention and is considered a promising direction of technological development.[12] Biometric recognition inherently possesses characteristics such as universality, distinctiveness, permanence, and collectability.[13] This allows the identification of individuals through unique biological characteristics inherent to each person, thus offering more stability compared with traditional methods since these characteristics do not change over time. Everyone can be rapidly and conveniently identified through their unique biological characteristics. Commonly used biological characteristics for identification include fingerprints, iris, face, and finger veins. Chen *et al.*[14] further categorized the areas for acquiring biometric features into internal and external biological characteristics. Identity recognition based on external biological characteristics such as fingerprints, palm prints, and face is already quite mature and can be found in applications such as smart lockers, mobile payments, smartphones, and access control systems. However, compared with internal biological characteristics, external ones are more susceptible to environmental factors, which may reduce the accuracy of biometric recognition. For example, fingerprint and palm print recognition can be affected by wounds, grease, or dirt on the fingers, impacting its accuracy.[15] Moreover, owing to the COVID-19 pandemic, people have grown concerned about techniques requiring physical contact for identity verification, fearing an increased risk of infection.[16] Consequently, facial recognition, which does not require physical contact and has lower levels of interference, has been adopted in many studies on identity verification for online courses.[17] However, facial recognition is highly sensitive to variations in gender, occlusion, head pose, illumination, and facial expression, which can reduce its accuracy.[18] Additionally, students' privacy concerns have been increasingly highlighted in recent years, with face-based identity recognition criticized for potentially invading privacy rights, making it difficult to promote in educational fields.[19] In summary, external biometric features are more vulnerable to environmental influences, leading to instability in practical

applications. Moreover, biometric recognition based on external features often involves physical contact and privacy issues, which could hinder its adoption in the educational sector. In contrast, veins represent a more stable internal biological characteristic. They are hidden under the skin, making them difficult to steal or forge; furthermore, they do not wear or change with age. However, vein-based biometric recognition still has drawbacks that are mainly related to the method of vein image acquisition. Because low-cost near-infrared (NIR) cameras are most frequently used, capturing vein images is affected by lighting conditions and user behavior, leading to issues with image quality due to illumination variations, vein translation, and rotation.

To address the issues of vein imaging mentioned above and to simultaneously lessen the weight of the model for practical application in real-world environments, we introduce a lightweight dual-attention convolutional neural network (LDA-FV), constructed by stacking dual-attention-based inverted residual blocks (DA-IRBs), for finger-vein recognition. In this approach, DA-IRB first utilizes a spatial attention mechanism (SAM) to perceive important features within the finger-vein image. It then employs a series of convolution operations to extract distinctive finger-vein texture features. Following this, a channel attention mechanism (CAM) is used to weigh the mapped high-dimensional finger-vein features, facilitating feature selection for finger veins. Through the method proposed in this study, the model can significantly reduce the number of parameters while maintaining the same level of accuracy. This not only lowers the deployment cost of the model but also allows for the flexible deployment of finger vein recognition across various hardware devices in distance education, thereby effectively enhancing the quality of teaching in distance education. To further enable the model to identify individuals based on their finger-vein features, we incorporate an adaptive margin loss (AML) function.[20] This function prompts the model to adjust the training difficulty in accordance with the image quality and simultaneously enhances the model's generalization ability. The method proposed in this study is aimed at creating an effective and efficient system for finger-vein recognition, adaptable to various qualities of vein images in practical scenarios. The main contributions of this study are as follows.

DA-IRB is incorporated to enhance the model's feature extraction capabilities, which allows the finger-vein recognition model to focus on important texture features within finger-vein images, enabling it to learn more distinctive features and simultaneously increase its recognition ability.

A lightweight LDA-FV model for finger-vein recognition is proposed in this study. It is constructed by consecutively stacking DA-IRBs. Furthermore, AML is employed to enhance the model's feature extraction capability from finger-vein images of different qualities. The experimental results showed that the LDA-FV model not only outperformed previous methods in finger-vein recognition using the finger-vein database of the University Sains Malaysia (FV-USM) and the PLUSVein dorsal-palmar finger-vein (PLUSVein-FV3) public database but also maintained a lower number of parameters.

The LDA-FV model used for finger-vein recognition provides a secure and efficient identity recognition technology for distance education, further improving the quality and fairness of distance education. This improvement enhances the foundational infrastructure of existing distance education.

2. Related Work

In recent years, numerous methods for finger-vein recognition have been proposed to address the challenges associated with vein imaging. Liu *et al.*[12] proposed a multiscale and multistage residual attention network (MMRAN) for finger-vein recognition. However, they used a batch size of less than 8 for model training, hindering the effectiveness of batch normalization (BN) and possibly leading to a degradation in the model's recognition capability.[21] Bilal *et al.*[22] utilized traditional CV algorithms for image enhancement of finger-vein images before feeding them into a convolutional neural network (CNN) for recognition. However, the image enhancement processing they used tended to severely damage vein features, thereby limiting the CNN model's recognition ability. Al-Tamimi and AL-Khafaji[23] employed a contrast-limited adaptive histogram (CLAHE), median filtering, and principal component analysis (PCA) for image enhancement, followed by training of a CNN with both pre- and postenhanced images. However, using CLAHE for enhancing vein images created inconsistent illumination, which in turn restricted the model's recognition capability.[24] Zhang *et al.*[25] introduced the histogram of oriented physiological Gabor responses (HOPGR) for finger-vein recognition. While effective in addressing finger tilt issues, this method struggled with finger bending or longitudinal finger rotation, potentially leading to reduced identification accuracy. Zhang *et al.*[26] also proposed an adaptive Gabor CNN (AGCNN) for finger-vein recognition, aiming to solve the issue of large parameter sizes and computational demands typically found in neural networks. Even though their AGCNN model utilized three linear layers as classifiers, it still had a large number of parameters and was prone to overfitting on finger-vein training datasets. Liu *et al.*[27] introduced a novel CNN architecture for finger-vein recognition, comprising two different branches: a trunk branch using residual units for feature extraction, and a soft mask branch using an hourglass network for global vein feature extraction. The complexity of this architecture, however, resulted in a high number of model parameters, potentially limiting its deployment in real-world scenarios owing to hardware constraints. Chai and co-workers[28,29] also used parts of the MobileNetV2 architecture as the main model for extracting finger-vein features. In their former study,[28] they used convolutional layers for feature extraction and global average pooling (GAP) to transform vein features into one-dimensional feature vectors to avoid a large increase in model parameters from subsequent linear layers. However, the high channel dimensions of the model led to a rapid increase in the number of parameters, making it a challenge to maintain a lightweight model. They then addressed this issue by reducing the channel dimensions of the model and simultaneously using automatic color enhancement (ACE) for image enhancement to improve the generalization ability of the finger-vein recognition model;[29] however, their ACE method had a high computational complexity, making it difficult to apply in real-world model deployments.

3. Proposed Method

In this study, we propose a finger-vein recognition model architecture, LDA-FV, constructed by continuously stacking DA-IRBs, as shown in Fig. 1. The LDA-FV architecture not only effectively extracts finger-vein texture features and improves the model's correct identification

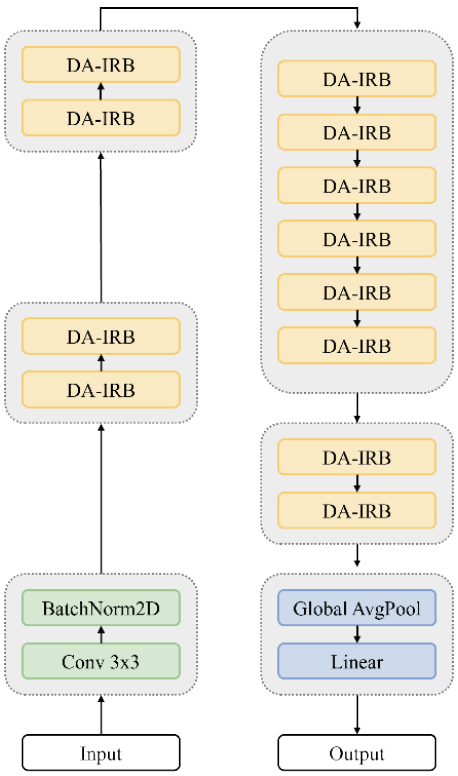

Fig. 1. (Color online) Block diagram of architecture of the proposed LDA-FV.

rate (CIR), but also reduces the number of the model's parameters through the lightweight structure of the DA-IRB. This approach is designed to meet the requirements of practical finger-vein recognition applications. In the following sections, a detailed description of the DA-IRB proposed in this study and the technical methods employed are discussed.

3.1 Dual-attention-based inverted residual block

To address past issues with finger-vein recognition and achieve a lightweight model, in this study, inspired by the design philosophy of ConvNeXt,[30] we employed a DA-IRB effectively designed for extracting finger-vein texture features, as shown in Fig. 2(a). The DA-IRB in this study uses a SAM to extract finger-vein feature maps from large-scale feature maps, enabling the model to effectively perceive and locate areas of finger-vein texture features. After extracting features with SAM, DA-IRB employs a 7 × 7 depthwise convolution (DWconv)[31] with a large convolution kernel to extract distinctive texture features on the basis of important finger-vein texture areas perceived by SAM. This also compensates for the insufficient effective receptive field associated with smaller convolution kernels.[32] The SAM[33] is represented by two vectors in different directions, where each element in the vectors reflects whether the object of interest appears in the corresponding row or column, as shown in Fig. 2(b). Hence, the integration of the SAM architecture into the DA-IRB significantly improves the finger-vein recognition model's

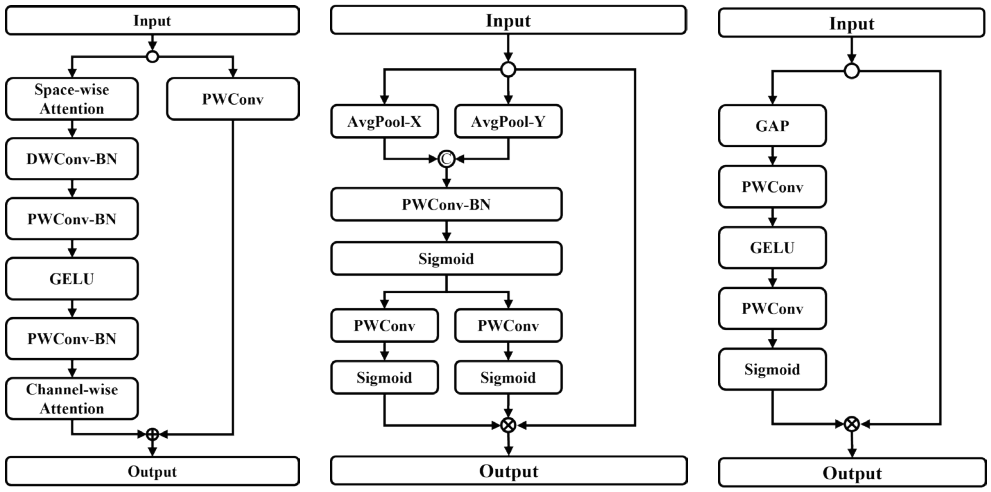

(a) (b) (c)

Fig. 2. The architectures of (a) DA-IRB proposed in this study, (b) SAM used in DA-IRB, and (c) CAM used in DA-IRB.

capability to detect essential finger-vein texture features in spatial dimensions. Additionally, it facilitates the efficient extraction of features utilized for identity recognition. Following this, adhering to ConvNeXt's design guidelines, DA-IRB uses two consecutive pointwise convolutions (PWConv) to expand and then map the channel dimensions of the finger-vein feature maps, preventing loss of feature information owing to dimension reduction. Finally, the DA-IRB module uses a CAM[34] to perform channel weighting on the previously extracted finger-vein feature maps, enabling the model to perceive which channels contain important finger-vein features and filter out insignificant channel features to avoid unnecessary focus. The CAM, depicted in Fig. 2(c), compresses the spatial information of the feature map into one-dimensional channel features using GAP and then squeezes and excites the channel dimensions through consecutive convolutional layers. This recalibrates the channel features of the model, enhancing its feature extraction capability. By integrating CAM into the DA-IRB, the finger-vein recognition model becomes more focused on crucial channel features and improves its capability to represent finger-vein characteristics. Combining the aforementioned two types of attention mechanisms, the DA-IRB improves the finger-vein model's ability to extract important, subtle texture features and accurately filters the extracted finger-vein features. This approach helps to avoid the model's focus on areas irrelevant to identity recognition, while simultaneously strengthening its ability in identity recognition. Furthermore, to effectively transform low-level texture features into high-level semantic features for classification, we constructed each stage of the model with a module ratio of 1:1:3:1.

3.2 Adaptive margin loss function

In practical applications, finger-vein recognition models may encounter low-quality and blurry vein images, making it challenging for the model to extract finger-vein features and

identify individuals, thereby raising concerns about the practical application of finger-vein recognition. To tackle this concern, we employed an AML approach, allowing the model to train independently in accordance with the quality of distinct finger-vein images. The AML function uses an image quality indicator to help the model identify low-quality images. The higher the value of this indicator, the better the quality of the image. The calculation of this indicator is shown as

$$\widehat{\|z_i\|} = \left\lfloor \frac{\|z_i\| - \mu_z}{\sigma_z / h} \right\rceil_{-1}^{1}, \tag{1}$$

where μ_z and σ_z represent the mean and standard deviation used to statistically analyze all features within the same batch, respectively. The operation $\lfloor \cdot \rceil$ is employed to clip the feature values to an interval between 1 and −1, while simultaneously avoiding their inclusion in gradient calculations. Meanwhile, h is used to keep the normalized values within the 1 to −1 interval to prevent excessive clipping of values. By normalizing the deep features $\|z_i\|$ outputted by the model and clipping the values, the feature distribution of $\|z_i\|$ is forced to approximate a Gaussian distribution, ensuring that the values are distributed within the 1 to −1 interval. However, to adapt the model to varying levels of difficulty among samples on the basis of image quality, two types of margin values, g_{angle} and g_{add}, are calculated from the values obtained in Eq. (1), as shown in Eq. (2). In this approach, a higher image quality resulted in smaller g_{angle} and larger g_{add} values. On the other hand, poorer image quality led to a greater g_{angle} value and lower g_{add} value.

$$\begin{cases} g_{angle} = -m \cdot \widehat{\|z_i\|} \\ g_{add} = m \cdot \widehat{\|z_i\|} + m \end{cases} \tag{2}$$

Once the margin values are calculated using Eq. (2), they are then incorporated into the AML, as shown in Eq. (3). The AML function adjusts the training difficulty on the basis of the quality of the image. When the image quality is poor, the loss function does not increase the training difficulty for that feature and when the image quality is better, the loss function significantly increases the training difficulty for the feature by using the margin values.

$$L_{AML} = -\log \frac{\exp\left(s\left(\cos\left(\theta_j + g_{angle}\right) - g_{add}\right)\right)}{\exp\left(s\left(\cos\left(\theta_j + g_{angle}\right) - g_{add}\right)\right) + \sum_{j \neq y_i}^{C} \exp\left(s\cos\theta_j\right)} \tag{3}$$

4. Experimental Results and Comparison

To evaluate the finger-vein recognition capabilities of the LDA-FV model, we utilized FV-USM[35] and PLUSVein-FV3[36] public databases for training. The FV-USM database contains data from 123 subjects and is a collection of 5904 NIR finger-vein images with a resolution of 640 × 480. For each subject, images of the left forefinger, left middle finger, right forefinger, and right middle finger were collected. The vein images from different fingers are considered distinct categories. The PLUSVein-FV3 database includes data from 60 subjects. Kauba *et al.*[36] used NIR LED and laser sensors to collect 7200 palmar and dorsal finger-vein images, each with a resolution of 1280 × 1024. Vein images from different sides (palmar and dorsal) are considered different subsets. For a fair comparison with past research results, in this study, we only used the palmar side finger vein images captured with LED and laser sensors for model evaluation. Before model training, we divided the FV-USM and PLUSVein-FV3 databases into training, validation, and test sets for model evaluation, with dataset ratios of 4:1:1 and 3:1:1, respectively. In terms of hyperparameter settings, the initial learning rate was set to 0.001, the image size to 112, the batch size to 32, and the number of epochs to 40. AdamW[37] and cosine annealing were chosen as the optimizer and learning rate scheduler, respectively, for model training. Finally, the proposed model was trained using the PyTorch Toolbox on a computer with a 12th Gen Intel® Core™ i9-12900H CPU and an Nvidia RTX 3080 Ti graphics processing unit. To assess the feasibility of the lightweight LDA-FV model architecture proposed in this study, the FV-USM database was used to evaluate the overall performance of the model. The model's security was measured using the *CIR* metric. A high value of this metric indicates high security and better overall system recognition performance, making it suitable for one-to-many finger-vein recognition tasks. The calculation of *CIR* is described as

$$CIR = \frac{Correction\ case}{Number\ of\ total\ case}. \tag{4}$$

The experimental results show that the LDA-FV model architecture proposed in this study achieved a high *CIR* of 99.90% on the FV-USM database, with a total of 1.2 million model parameters. Compared with methods proposed in other studies, the LDA-FV model architecture not only had fewer model parameters but also maintained higher accuracy, as shown in Table 1. Furthermore, to validate the generalization of the LDA-FV model in finger-vein recognition, a comparative analysis was conducted using the PLUSVein-FV3 database. The results showed that the LDA-FV model achieved *CIR*s of 97.50% and 97.22% on images captured by LED and laser sensors, respectively, in the PLUSVein-FV3 database, as indicated in Table 2. It is noteworthy that the LDA-FV model architecture in this study, compared with the previous FV-RSA model, not only had similar *CIR* but also had a lower number of model parameters. This significant reduction in computational complexity makes the deployment of the LDA-FV model in real-world environments feasible. Additionally, compared with the previous ILCNN model, the LDA-FV achieved higher *CIR* values on both the FV-USM and PLUSVein-FV3 databases and had a

Table 1
Results for proposed model and from previous research on the FV-USM database.

Methods	CIR (%)	Params (M)
Semi-PFVN[28]	94.67	3.35
MMRAN[12]	96.07	3.51
LightFVN + ACE[29]	96.17	2.65
W. Liu *et al*.[27]	98.58	5.85
LFVRN_CE + ACE[24]	99.09	4.93
EfficientNet-B0[38]	99.70	4.64
ILCNN[39]	99.82	1.23
FV-RSA[40]	**99.90**	8.70
LDA-FV (This work)	**99.90**	**1.20**

Table 2
Results for proposed model and from previous research on the PLUSVein-FV3 database.

Methods	CIR (%)	
	LED	Laser
DenseNet-121[41]	93.06	93.19
EfficientNet-B0[38]	95.82	92.22
ILCNN[39]	95.90	93.52
LDA-FV (This work)	**97.50**	**97.22**

lower number of model parameters. This improvement might have stemmed from the LDA-FV model's ability to map finger-vein features onto a higher channel dimension during the feature extraction process. This approach allowed the model to learn and filter finger-vein features more effectively, thereby achieving a higher *CIR* with fewer parameters.

5. Conclusions

In this study, we introduced a finger-vein recognition model architecture, LDA-FV, constructed by stacking lightweight DA-IRBs equipped with attention mechanisms. The performance of this model architecture was comprehensively evaluated using the FV-USM and PLUSVein-FV3 public databases. The DA-IRB architecture in this study enabled the LDA-FV model to effectively perceive important regions of finger-vein texture features and selectively filter features in these areas. This ensured that the extracted finger-vein textures were beneficial for identity recognition, and also simultaneously enhanced the model's recognition capability. As illustrated in the experimental results, the LDA-FV model not only achieved better *CIR* on both FV-USM and PLUSVein-FV3 databases compared with previous methods but also maintained a lower number of model parameters. This reduction in parameters means that the LDA-FV model is less constrained by hardware limitations and can more easily apply finger-vein recognition to practical distance education environments. Our results demonstrate the potential of the LDA-FV model in practical applications, which offers a balance between efficiency, accuracy, and ease of deployment in real-world environments.

References

1 SWP Report 2023: the problem with too few: https://www.unfpa.org/swp2023/too-few (accessed April 2023).
2 O. V. Pavlov and E. Katsamakas: PLoS One **15** (2020) e0236872. https://doi.org/10.1371/journal.pone.0236872
3 M.-Y. Hsieh: IEEE 3rd Eurasian Conf. Educational Innovation (IEEE, 2020) 909–911.
4 M. Ciotti, M. Ciccozzi, A. Terrinoni, W.-C. Jiang, C.-B. Wang, and S. Bernardini: Crit. Rev. Clin. Lab. Sci. **57** (2020) 365. https://doi.org/10.1080/10408363.2020.1783198
5 Y.-K. Chan, M. Y. Hsieh, and M. Usak: Sustainability **13** (2021) 2203. https://doi.org/10.3390/su13042203
6 P. M. Newton and K. Essex: J. Acad. Ethics (2023). https://doi.org/10.1007/s10805-023-09485-5
7 A. Shata, Z. N. Haitaamar, and A. Benkrid: Int. Conf. IT Innovation and Knowledge Discovery (IEEE, 2023) 1–5.
8 F. Ozdamli, A. Aljarrah, D. Karagozlu, and M. Ababneh: Sustainability **14** (2022) 13230. https://doi.org/10.3390/su142013230
9 S. Maghsudi, A. Lan, J. Xu, and M. van der Schaar: IEEE Signal Process. Mag. **38** (2021) 37. https://doi.org/10.1109/MSP.2021.3055032
10 M. R. Mutizwa, F. Ozdamli, and D. Karagozlu: Trends High. Educ. **2** (2023) 16. https://doi.org/10.3390/higheredu2010002
11 F. Boutros, N. Damer, F. Kirchbuchner, and A. Kuijper: IEEE/CVF Conf. Computer Vision and Pattern Recognition Workshops (IEEE, 2022) 1578–1587.
12 W. Liu, H. Lu, Y. Wang, Y. Li, Z. Qu, and Y. Li: Appl. Intell. **53** (2023) 3273. https://doi.org/10.1007/s10489-022-03645-7
13 C.-H. Hsia and C.-H. Liu: IEEE Sens. J. **22** (2022) 13612. https://doi.org/10.1109/JSEN.2022.3177472
14 Y.-Y. Chen, C.-H. Hsia, and P.-H. Chen: IEEE Access **9** (2021) 149796. https://doi.org/10.1109/ACCESS.2021.3124631
15 Y.-Y. Chen, S.-Y. Jhong, C.-H. Hsia, and K.-L. Hua: ACM Trans. Multim. Comput. Commun. Appl. **17** (2021) 1. https://doi.org/10.1145/3468873
16 K. Okereafor, I. Ekong, I. O. Markson, and K. Enwere: JMIR Biomed. Eng. **5** (2020) e19623. https://doi.org/10.2196/19623
17 D. Joshi, P. Patil, V. Singh, A. Vanjari, T. Shinde, and H. Giri: 2023 5th Biennial Int. Conf. Nascent Technologies in Engineering (IEEE, 2023) 159–166.
18 V. Albiero, K.S. Krishnapriya, K. Vangara, K. Zhang, M. C. King, and K. W. Bowyer: IEEE/CVF Winter Conf. Applications of Computer Vision Workshops (IEEE, 2020) 81–89.
19 M. Andrejevic and N. Selwyn: Learn. Media Technol. **45** (2020) 115. https://doi.org/10.1080/17439884.2020.1686014
20 M. Kim, A. K. Jain, and X. Liu: IEEE/CVF Conf. Computer Vision and Pattern Recognition (IEEE, 2022) 18750–18759.
21 P. Luo, R. Zhang, J. Ren, Z. Peng, and J. Li: IEEE Trans. Pattern Anal. Mach. Intell. **43** (2021) 712. https://doi.org/10.1109/TPAMI.2019.2932062
22 A. Bilal, G. Sun, and S. Mazhar: J. Chin. Inst. Eng. **44** (2021) 407. https://doi.org/10.1080/02533839.2021.1919561
23 M. S. H. Al-Tamimi and R. S. S. AL-Khafaji: Int. J. Nonlinear Anal. Appl. **13** (2022) 3667. https://doi.org/10.22075/ijnaa.2022.6145
24 Y. Zhong, J. Li, T. Chai, S. Prasad, and Z. Zhang: Chinese Conf. Biometric Recognition (Springer, 2021) 295–303.
25 L. Zhang, W. Li, X. Ning, L. Sun, and X. Dong: Int. Conf. Pattern Recognition (IEEE, 2020) 4873–4878.
26 Y. Zhang, W. Li, L. Zhang, X. Ning, L. Sun, and Y. Lu: Concurr. Comput. Pract. Exp. (Wiley, 2020) 1–11.
27 W. Liu, H. Lu, Y. Li, Y. Wang, and Y. Dang: Chinese Conf. Biometric Recognition (Springer, 2021) 231–239.
28 T. Chai, J. Li, S. Prasad, Q. Lu, and Z. Zhang: J. Inf. Secur. Appl. **67** (2022) 103211. https://doi.org/10.1016/j.jisa.2022.103211
29 T. Chai, J. Li, Y. Wang, G. Sun, C. Guo, and Z. Zhang: Neural Process. Lett. **55** (2023) 2305. https://doi.org/10.1007/s11063-022-10937-z
30 Z. Liu, H. Mao, C.-Y. Wu, C. Feichtenhofer, T. Darrell, and S. Xie: IEEE/CVF Conf. Computer Vision and Pattern Recognition (IEEE, 2022) 11976–11986.
31 M. Sandler, A. Howard, M. Zhu, A. Zhmoginov, and L.-C. Chen: IEEE Conf. Computer Vision and Pattern Recognition (IEEE, 2018) 4510–4520.
32 X. Ding, X. Zhang, J. Han, and G. Ding: IEEE/CVF Conf. Computer Vision and Pattern Recognition (IEEE, 2022) 11963–11975.

33 Q. Hou, D. Zhou, and J. Feng: IEEE/CVF Conf. Computer Vision and Pattern Recognition (IEEE, 2021) 13713–13722.
34 J. Hu, L. Shen, and G. Sun: IEEE Conf. Computer Vision and Pattern Recognition (IEEE, 2018) 7132–7141.
35 M. S. M. Asaari, S. A. Suandi, and B. A. Rosdi: Expert Syst. Appl. **41** (2014) 3367. https://doi.org/10.1016/j.eswa.2013.11.033
36 C. Kauba, B. Prommegger, and A. Uhl: Int. Conf. the Biometrics Special Interest Group (IEEE, 2018) 1–5.
37 I. Loshchilov and F. Hutter: IEEE Conf. Learning Representations (IEEE, 2019).
38 M. Tan and Q. V. Le: Int. Conf. Machine Learning (IEEE, 2019) 6105–6114.
39 C.-H. Hsia, L.-Y. Ke, and S.-T. Chen: Bioengineering **10** (2023) 919. https://doi.org/10.3390/bioengineering10080919
40 Z. Zhang, G. Chen, W. Zhang, and H. Wang: IEEE Access **12** (2023) 1943. https://doi.org/10.1109/ACCESS.2023.3347922
41 G. Huang, Z. Liu, L. V. D. Maaten, and K. Q. Weinberger: IEEE Conf. Computer Vision and Pattern Recognition (IEEE, 2017) 4700–4708.